# History of the Concept of Cloud-Defined Weather States or Cloud Regimes

William B. Rossow
May 2022

Atmospheric motions are produced by an inhomogeneous distribution of heating by several processes: radiation, precipitation and sensible heat flux from the surface. The vertical component of these motions produces clouds, which induce heating perturbations by radiation and, particularly, by precipitation (some clouds are produced by radiative cooling) that feedback on the motions. This tight feedback loop is difficult to diagnose because the interactions occur over the whole range of the space-time scales of atmospheric motions. Especially lacking are measurements over the whole range of scales of the vertical motions that form the clouds. The usual observation-based approach is to measure and analyze the (usually time-averaged, essentially) static properties of the atmosphere and associated cloud properties or morphological types. This approach does not capture the dynamic relationships or their variations with scale. Ground-based measurements do not cover the relevant range of spatial scales, aircraft-based measurements do not capture the time variations, and satellite-based measurements, while covering the range of both space and time variations, are very limited in what properties of the clouds and atmosphere they measure (especially at higher time resolution). Satellite imaging instruments can cover the space-time range of cloud variation scales, but measure only a few properties (at cloud top), whereas profiling instruments do not (yet) provide complete coverage of the relevant time scales.

The idea of distinct atmospheric conditions or states naturally arises in the contrast between fair and foul weather, especially since "stormy" weather is fortunately relatively rare. Cloud properties or types have long been associated with changing weather conditions; for example Lau and Crane (1995, 1997) specifically associate the spatial distribution of cloud types from satellite and surface observations within tropical and extratropical storms (see also Fig. 5 in Rossow *et al.* 2005a). This concept has been extended to encompass atmospheric dynamical regimes; for example, Michelangeli *et al.* (1995) compare different ways to classify the midlatitude patterns of geopotential height. Lorenz (1984) even demonstrated that a simple atmospheric model chaotically transitions between distinctly different states.

Two concepts from quantum mechanics also suggest a cloud process analysis approach. The first concept is to represent the continuum of atmospheric conditions and associated cloud properties by a small set of (approximately) “discrete” states and represent the time variations as transitions among these states. These “weather states” (WS) collapse multi-variate relationships into a simpler representation of the time derivatives of cloud dynamical processes focusing on their bulk attributes. The second concept is to search for statistical (probabilistic) relationships between these states and the properties of the larger scale atmospheric circulation. The transitions of one WS into another in time associated with changing atmospheric properties and motions can provide useful diagnostic and dynamic relationships. By defining the WS in terms of cloud structure patterns (frequency histograms of cloud properties over small domains), they

are proxies for the vertical motions that produce clouds: cloud top pressure (or height) distributions provide some indication of the vertical scale of the atmospheric motions and cloud optical thickness (or water path) provides some indication of the strength of the vertical motions producing the clouds. Thus, a diagnostic equation can be defined that relates the time variations of the cloud properties as represented by the WS to the time variations of the atmospheric conditions.

Although frequency histograms of satellite measurements have occasionally been used in analyses since the earliest days, recent research on cloud processes in weather and climate has employed a very particular approach that associates distinctive spatial patterns (at mesoscale, 100-300 km) in two-dimensional (joint, 2D) distributions of cloud properties with particular atmospheric conditions to investigate relationships that might reveal the links between atmospheric motions and the clouds they produce (Tselioudis *et al.* 2013, Rossow *et al.* 2016, Tselioudis *et al.* 2021). This is a reversal of the more common regime analyses, which define regimes based on properties and/or motions of the atmosphere, and look for the associated cloud properties. An early example of the more common approach using satellite data is Fu *et al.* 1990. More recent examples are papers by Marchand *et al.* (2006, 2008), Evans *et al.* (2012) and a series of papers, including Pope *et al.* 2009a,b, Protat *et al.* 2011, Raut *et al.* 2014. Marchand *et al.* (2006) notably describe a "high dimension" analysis method that classifies the atmospheric state using a large number of variables (shapes of vertical profiles); such an analysis method may be needed to extend the 2D-based results describe below. After brief mention of some early uses of satellite measurement histograms, this history focuses on the development and use of the particular concept of the 2D spatial frequency distribution patterns.

The use of 2D histograms of satellite-measured radiances in cloud studies began as soon as the first multi-wavelength satellite observations of Earth became available in the 1960s. Vonder Haar (1970) actually had to combine nearly-coincident visible wavelength photographs from one satellite (ESSA-IX) with infrared radiances from another satellite (NIMBUS-3) to discuss possible cloud type identifications in the joint images; he suggested a simple 4-part scene classification (bright-dark, cold-warm) that this combination made possible. By the 1970s and 1980s most satellite imagers had at least two channels, one at a visible wavelength (approximately 0.6 μm) and one at a window infrared wavelength (approximately 10.5 μm). The earliest METEOSATs had a third channel more sensitive to water vapor (see below). Starting in the 1980s with the polar orbiter imagers and then later with the geostationary imagers in the 1990s, more spectral channels were added, so that today these satellite imagers commonly have a dozen or more channels, making expanded higher-dimensional analyses possible.

Most of the first uses of 2D histograms in the 1970s and 1980s composed them directly from the visible-infrared radiances over various sized domains and divided the joint distributions in various ways to set cloud detection thresholds or to determine cloud cover directly (*e.g.*, Stamm and Vonder Haar 1970, Simmer *et al.* 1970, Shenk and Salomonson 1972, Phulpin *et al.* 1972, Desbois and Seze 1984, Minnis and Harrison 1984, England and Hunt 1985). Shenk *et al.* (1976) used pre-calculated radiance thresholds to divide a four-channel space (0.2-4.0, 6.5-7.0, 10-11, 20-23 μm from the MRIR on NIMBUS 3 with 55 km pixels) to define 10 cloud types or cloud type mixtures in 20 cases over open tropical ocean, essentially a scene classification method.

Four papers in the 1980s proposed using concentrations (clusters) within the radiance histograms to identify different cloud types. Desbois *et al.* (1982) actually used all three channels from METEOSAT, where the third channel (approximately 6.7 μm wavelength) provides better discrimination between low clouds and high transparent clouds. They associated different cloud types with different portions of the 3D frequency distributions (see also Desbois and Seze 1984, Seze and Desbois 1987). They did this by using an objective statistical procedure (the same as used in later papers) to find clusters within the 3D frequency distribution for image sectors defined by 200 by 200 pixels (a domain of about 1000 km): these clusters were identified as different cloud types (as well as the clear portions), which was used to determine cloud cover fraction. They interpreted the scattering of image pixels with radiances in between the clusters as representing mixtures of cloud types. Arking and Childs (1985), with a different third channel (approximately 3.7 μm wavelength that provides information about cloud particle sizes) on the polar orbiting AVHRR (TIROS-N), used the 2D visible-infrared radiance histograms in two ways. First, they identified clusters within the 2D distributions that they interpreted to represent pixels completely covered by clouds with particular properties (cloud types) and interpreted other in-between-cluster pixels as partially covered pixels (see also Platt 1983). Then they moved these pixels along theoretical trajectories, calculated by varying sub-pixel cloud cover fraction, until the clustering was maximized, and retrieved three cloud physical properties – one of the earliest examples of a physical retrieval – cloud top temperature, optical thickness and particle size for the cluster centers assuming complete cloud cover. Second, they suggested that these clusters within the histograms represented particular cloud types. Inoue (1987) also proposed a classification of tropical clouds based on two-dimensional radiance distributions, but composed of the IR brightness temperature at the shorter of two nearby wavelengths and the spectral difference of the two brightness temperatures (*cf.* Inoue *et al.* 2009). Rossow and Lacis (1990) discussed the results of physical retrievals of two cloud properties (cloud top height and optical thickness) from individual pixel radiances, assuming all pixels to be completely cloud covered, in terms of cloud types defined by dividing the joint distribution of the retrieved cloud properties, not the radiances: cloud top height from the IR and optical thickness from the VIS.

In the early planning for the International Satellite Cloud Climatology Project (ISCCP), it was suggested that 2D histograms of visible-infrared radiances be included in the data products to represent the smaller scale cloud property variations within small domains (250-500 km in size). The earlier results of Desbois *et al.* (1982, also Desbois and Seze 1984, Seze and Desbois 1987), Arking and Childs (1985, see also Platt 1983), and Inoue (1987) supported this suggestion. The identification of cloud types associated with particular combinations of visible-infrared radiances from these earlier studies also suggested using the amount and average retrieved physical properties (cloud top temperature/pressure from the infrared and optical thickness from the visible) as one way to represent cloud type variations. Thus, the ISCCP products reported the amount and average properties of cloud types defined by three ranges of cloud top pressure and three ranges of optical thickness (Rossow and Schiffer 1991, 1999). However, the potential of the more detailed information provided by frequency histograms (both 1-dimensional and 2-dimensional) led to their inclusion in the ISCCP products as well, but in terms of cloud properties instead of radiances: top pressure (seven intervals) from analysis solely of

infrared radiances for all times of day and joint cloud top pressure (seven intervals) – optical thickness (six intervals) from analysis of infrared-visible radiances during daytime.

The cloud type identifications from satellite measurements and their association with the classical morphological types were evaluated by comparison with tropical and extratropical storm composites of surface observations (Lau and Crane 1995, 1997) and against collocated and coincident surface observations of the classical morphological cloud types (Hahn *et al.* 2001). This cloud type approach continues today (*e.g.*, Kato *et al.* 2016). Gordon *et al.* (2005) apply a cluster analysis to time variations of the average infrared-visible radiances in a single grid box, which amounts to finding the dominant frequencies of occurrence of cloud types defined by the joint radiance values.

Rossow and Schiffer (1991) and Rossow and Cairns (1995) drew attention to the patterns in the 2-dimensional (2D) cloud property histograms in the ISCCP data products and suggested they might be indicative of regional atmospheric conditions. The concept is to associate distinctive mesoscale mixtures of cloud types, as represented by different patterns of the whole 2-dimensional distribution, with different atmospheric conditions, rather than identifying concentrations within the distributions of radiances or cloud properties as particular cloud types. In other words, the basic analysis object is the whole distribution at one time and place rather than dividing the distribution into parts (or cloud types).

Jakob and Tselioudis (2003) were the first to apply an objective pattern analysis to one year of the ISCCP-D 2D histograms (cloud top pressure, PC, versus optical thickness, TAU) in a study of clouds in the tropical western Pacific. They used the K-means cluster analysis scheme (Anderberg 1973), similar to that used by Desbois *et al.* 1982 (some alternate analysis methods are Mixture Modeling Clustering, Smyth *et al.* 1999, Neural Network-based Bootstrap method, Marchand *et al.* 2006, Simulated Annealing, Fereday *et al.* 2008, and Self Organizing Maps, MacDonald *et al.* 2016). These early results already distinguished between shallow and deep convection regimes as well as identifying two different deep convection regimes, one composed of scattered plumes with a mixture of cirrus and shallow cumulus, and another larger-scale organized convection with thick anvil clouds (see also a similar approach to analyzing ground-based radar with similar conclusions in Caine *et al.* 2009). Although their analysis method is similar to that employed by Desbois *et al*. 1982 to find concentrations within individual multi-dimensional distributions, the Jakob and Tselioudis analysis identifies similar two-dimensional patterns in many such distributions. The resulting patterns are referred to as Cloud Regimes (CR) or Weather States (WS).

Before outlining research results obtained using WS based on the ISCCP-D and other similar analyses, the following papers document the production of several different versions of the ISCCP-D Weather State datasets (all on a 2.5° equivalent equal-area grid at 3-hr intervals) that are available from

https://isccp.giss.nasa.gov/analysis/climanal5.html
or www.cessrst.org/rscg/products.html

The Tropical Weather State dataset (TWS) extended the analysis of Jakob and Tselioudis (2003) to the whole tropics (± 15° latitude) covering July 1983 thru (finally) December 2009 (Rossow *et al.* 2005b). This dataset also identifies two forms of deep convection (ordinary scattered plumes with cirrus and mesoscale-organized) and shows that the main

variation time scales of tropical deep convection (MJO, annual, ENSO) are clearly associated with the variations of the mesoscale-organized form of deep convection rather than the scattered form (see more detailed results discussed below). The Extended Tropical Weather State dataset (ETWS), with latitude coverage extended to ± 35° latitude over the same time period, includes more shallow cloud types and was first used by Mekonnen and Rossow (2011). They showed that the initiation of African Easterly Waves over eastern tropical Africa is associated with a transformation of a perturbation of the already-present scattered deep convection WS into the mesoscale-organized WS over the Ethiopian highlands. The cluster analysis was then applied to the northern and southern midlatitude zones (± 35-65° latitude), NHWS and SHWS, respectively. These two datasets, together with ETWS, were used by Oreopoulos and Rossow (2011) to document associated radiative effects, showing that the "stormy" WSs (containing deep, optically thick clouds) produce net radiative heating of the atmosphere in both the tropics and midlatitudes. Haynes *et al.* (2011) used SHWS to composite cloud vertical profile, precipitation and radiation measurements of cyclone-related clouds over the southern oceans, with certain WS occurring in distinctive parts of the storm (*cf.* Lau and Crane 1995, 1997). To improve the time resolution of the Weather State analysis from, effectively, daily intervals to 3-hr intervals, Tan and Jakob (2013) constructed the IR Weather State data (IRWS), covering ± 35° latitude, by compositing the 1D cloud top pressure histograms corresponding to the 2D-histogram WS. They showed that the increased time resolution now resolved the two oppositely propagating components of an MJO event as the two forms of deep convection identified by the WS. A single global analysis by Tselioudis *et al.* (2013) produced the Global Weather State dataset (GWS) and showed the correspondence of the WS with cloud vertical structure from CloudSat/CALIPSO, radiation and the large-scale circulation (vertical motions). Another global analysis based on MODIS cloud products was produced by Oreopoulos *et al.* (2014) showing that the WS that predominate in producing precipitation also produce net radiative heating of the atmosphere.

A revised version of the ISCCP cloud products, called ISCCP-H (Young *et al.* 2018, Rossow *et al.* 2022), has now been produced and extending the time record (currently through 2018); a global Weather State dataset (GWS-H) has been produced by Tselioudis *et al.* (2021) on a 1.0° equivalent equal-area grid at 3-hr intervals covering July 1983 – December 2018 available from

https://isccp.giss.nasa.gov/analysis/climanal5.html

The following summarizes a chronology of research conducted using the ISCCP WS data products. Jakob *et al.* (2005) and Jakob and Schumacher (2008) expanded on the initial analysis of Jakob and Tselioudis (2003) by compositing precipitation, radiative fluxes and atmospheric temperature-humidity profiles from satellites and surface sites to establish that the WS actually do indicate different conditions in the tropical atmosphere and that, though more than one regime includes some deep convection, the preponderance of the precipitation is associated with one particular WS corresponding to the mesoscale-organized convection. At this stage, two tropical deep convection regimes had been recognized: one composed of scattered convective plumes mixed with cirrus and some shallow clouds, producing only modest precipitation and radiative perturbations, and one larger-scale, organized convection (actually represented by two WS in the TWS dataset, convection and precipitating anvil, that vary together) that

produces much more precipitation and much larger radiative heating of the atmosphere. The former is associated with atmospheric conditions that are only weakly unstable and moist whereas the latter is associated with stronger instability and more moisture.

Tromeur and Rossow (2010) used the WS state compositing approach to diagnose the properties and energy-water exchanges of MJO events, in particular identifying the distinctive switching of the type of deep convection from scattered, isolated systems to mesoscale-organized systems as the key signature of such events. Tselioudis *et al.* (2010) showed that the recently identified trend in stratospheric water vapor was correlated with a similar trend in the organized form of tropical deep convection identified by the TWS but not the other form of deep convection. Tselioudis and Rossow (2011) showed that it is the organized convection that exhibits the characteristic seasonal and ENSO variations in the tropics. Meknonnen and Rossow (2011) showed that the same switching of deep convection from scattered to mesoscale organized form near the Ethiopian mountains was associated with the onset of heavy precipitation and initiation African Easterly Waves.

Oreopoulos and Rossow (2011) documented the radiative effects of the clouds associated with tropical and midlatitude WS, showing that the storms (systems producing precipitation) are also the WS that produce radiative heating of the atmosphere. Haynes *et al.* (2011) showed that the southern midlatitude WS appear in distinctive portions of cyclonic systems (indicated by surface low pressure anomalies), extending the earlier results of Lau and Crane (1995, 1997).

Tselioudis *et al.* (2013) developed a global set of WS and showed that these corresponded with not only the vertical motions of the large-scale atmospheric circulation but also exhibited distinctive cloud vertical structures as observed by CloudSat and CALIPSO.

Tan *et al.* (2013) continued the analysis of the properties of different types of tropical convection, showing more details from sub-dividing the WS. Li *et al.* (2013) evaluated tropical atmospheric radiative heating by upper-level clouds, identified by TWS, by matching with radiative flux profiles based on CloudSat/CALIPSO cloud profiles, finding the column-integrated magnitude to be dominated by the mesoscale-organized systems. Rossow *et al.* (2013) and Lee *et al.* (2013) examined the composite precipitation amounts associated with the tropical WS, showing in particular that the mesoscale-organized form of deep convection is not only responsible for most of the total precipitation but also solely responsible for the extreme precipitation events, thereby extending the earlier results for the western Pacific (Jakob *et al.* 2005, Jakob and Schumacher 2008, see also the papers discussed below by Pope *et al.* 2009a,b and Protat *et al.* 2011) to the whole tropics. Stachnik *et al.* (2013) composited sounding-based estimates of the apparent heat source and moisture sink from a variety of field campaigns by WS and found the strongest heating/drying associated with the mesoscale-organized convection and the strongest cooling/moistening associated with WS dominated by low-level clouds and clear sky. Handlos and Back (2014) extended the analysis of the association of atmospheric conditions and tropical WS to show that diagnosed vertical profiles of vertical velocity also were distinctively different among the WS; in particular the mesoscale type of deep convection exhibited a strong ascent in the upper troposphere but offsetting descent in the lower troposphere associated with the mesoscale anvil circulation.

Mason et al (2014) combine reanalysis and CloudSat/CALIPSO cloud profiles to refine the vertical distribution of clouds from the SHWS to extend the analysis of Haynes *et al.* (2011) to identify in more detail the kinds of mid-topped clouds present at high southern latitudes that might explain model deficiencies in solar fluxes there.

Tan *et al.* (2015) showed that the recent indications of trends in tropical precipitation amounts (regionally of both signs) are explained solely by trends in the frequency of occurrence of the mesoscale organized form of deep convection identified by the WS (consistent with the overall trend in stratospheric water vapor, Tselioudis *et al.* 2010).

All these results demonstrated that the ISCCP-based WSs correspond to distinctive atmospheric properties, circulation, radiation, precipitation and cloud vertical structures.

Oreopoulos *et al.* (2014) developed a set of WS (called Cloud Regimes) by applying to MODIS cloud products the same analysis procedures as Jakob and Tselioudis (2003) and demonstrated similar associations with cloud vertical structure, radiative perturbations and precipitation, as well as the large-scale atmospheric properties and circulation. Oreopoulos *et al.* (2016) updated the previous results using a more recent version of the MODIS cloud products and focused on more detailed examination the composite radiative effects associated with the WS from three different radiative flux products. The comparison of the MODIS-based and ISCCP-based WS shows that there are some differences of the definition of the WS based on different choices of criteria and the cloud retrieval methods, mostly involving "marginal" clouds such as thin cirrus and clouds in the polar regions (the MODIS data have less thin cirrus than the ISCCP data); however the correspondence of the WS with distinctive atmospheric properties, circulation, radiation, precipitation and cloud vertical structures are all confirmed. Leinonen *et al.* (2016) found regional variations of CloudSat/CALIPSO cloud vertical distributions and radiation/precipitation that are labeled as the same MODIS WS from a global analysis (although they did not consider whether an analysis of the WS by region would have provided a better correspondence among these observations). Oreopoulos *et al.* (2017a) re-analyzed the MODIS-based WS composites of atmospheric properties, precipitation and radiation sorted by estimates of aerosol amount to look for any systematic dependence that might be ascribed to aerosol effects on clouds (see also Malavelle *et al.* 2017 and Oreopoulos et al. 2020). Oreopoulos *et al.* (2017b) extended the analysis of Tselioudis *et al.* (2013) to the correspondence of MODIS-WS and CloudSat/CALIPSO cloud vertical structures. Tan and Oreopoulos (2019) composited a new high space-time resolution precipitation dataset with MODIS-based WS to examine the sub-grid variability and fractional coverage for the different types of cloud systems, showing that fractional coverage and grid-averaged precipitation tend to increase together. Jin *et al.* (2020) examined the spatial structures of large convective systems in terms of WS variations. Cho *et al.* (2021) describe an updated version of their results for the latest version of MODIS cloud products.

Rossow *et al.* (2016) extended the previous analyses to quantify the composite diabatic heating of the atmosphere associated with each of the global ISCCP-D WS and showed that the energy balance of each climate zone is characterized by different WSs, one very infrequent WS providing the atmospheric heating by both precipitation and radiation and one more persistent WS providing the radiative cooling. Mekonnen and

Rossow (2018) employed the higher time resolution IRWS to clearly establish that the change of deep convection style from disorganized to organized triggers the AEW. Worku *et al.* (2019, 2020) used the IRWS dataset to document the diurnal variations of deep convection over the Maritime Continent and to diagnose the interaction of the diurnal variations with a passing MJO event.

There are some analyses of cloud-defined regimes that use satellite measurements other than visible-infrared radiances described above. Liu *et al.* (1995) combined infrared with microwave radiances with a particular focus on precipitating cloud systems. Zhang *et al.* (2007) applied a pattern analysis to CloudSat radar profiles to categorize the shapes of radar reflectivity with height (see Pope *et al.* 2009a,b for a similar analysis using ground-based radar). Mace and Wrenn (2013) also evaluated the ISCCP WS using CloudSat and CALIPSO. Related to clouds are regimes defined by patterns in satellite precipitation profiles, such as Boccippio *et al.* (2005), who applied a profile classification to the TRMM precipitation radar profiles (*cf*. Yuter and Houze 1995, Caine *et al.* 2009 for examples of similar analyses using ground-based radar). Luo *et al.* (2017) extended the WS-type analysis to combined TRMM, CloudSat and CALIPSO profiles of cloud and precipitation establishing a firm connection with the WS based on ISCCP cloud properties. Unglaub *et al.* (2020) also analyzed the combined CloudSat and CALIPSO cloud profile data.

Several studies have employed the WS results from satellites to evaluate climate models (Williams and Tselioudis 2007, Williams and Brooks 2008, Williams and Webb 2009, Chen and Del Genio 2009, Tsushima *et al.* 2013, Bodas-Salcedo *et al.* 2014, Mason *et al.* 2014, Remillard and Tselioudis 2015, Jin *et al.* 2017, Tan *et al.* 2018, Tselioudis *et al.* 2021). Needless to say, the comparisons show a wide range of model "skill" in representing clouds and their processes.

McDonald *et al.* (2016) apply a different classification approach to the ISCCP-D data than the above discussed papers but obtain broadly similar, although more detailed, results (McDonald *et al.* 2018 compare the two types of pattern analysis). Results from this type of analysis have also been compared with models (Schuddeboom *et al.* 2018).

Another approach to relating clouds and other atmospheric attributes is to classify the atmospheric properties and form a composite of cloud properties − the opposite approach to the WS analysis. Such dynamical composites of cloud properties have also been performed (Tselioudis *et al.* 2000, Bony *et al.* 2004, Su *et al*. 2008, Haynes *et al,* 2011, Li *et al.* 2014, Polly and Rossow 2016). To investigate these kinds of results further, the results of cloud-classified dynamical composites and dynamics-classified cloud composites need to be compared. McDonald *et al.* (2018) have started on this; for the simple one-parameter representation of dynamics (500 hPa vertical velocity), they find that the WS to provide more discrimination. Gryspeerdt *et al.* (2014) use a similar approach to evaluate aerosol effects. However, a more complete representation of the atmospheric state (multiple variables) may improve the relationships. Williams and Bodas-Salcedo (2017) combined the two approaches in comparisons of observations with models.

There now two versions of the global ISCCP WS, one based on ISCCP-D on a 2.5° equal-area grid (Tselioudis *et al.* 2013) and another based on ISCCP-H on a 1.0° equal-area grid (Tselioudis *et al.* 2021): these two WS datasets, along with a table comparing their average properties, and their geographic distributions (relative frequency

of occurrence, RFO) are shown below. Also shown are the composite cloud vertical structures from collocated and coincident CloudSat and Calipso observations. In general the results are very similar but the H-version WS are a little "cleaner" and "simpler" in several respects. In GWS-H, (1) the deep convective part of WS3 moved to DCN (deep convection), better isolating deep convection in the tropics (although losing the distinction of convective types), and the cirrus part of WS3 combined with WS6 into CIR, (2) the cirrus part of WS5 moved from the corresponding MID (mid-level) to CIR, (3) MID has more true mid-level cloudiness, (4) the thinner, more scattered cumulus moved from WS8 to FRW (fair weather), (5) SHC (shallow cumulus) combined the remainder of WS8 with WS9 and is better confined to the equatorward part of the midlatitude storm tracks, (6) and STC (stratus) combined WS10 and WS11 and is better confined to the subtropics. These changes are reflected in simpler composite vertical structures. Because of the smaller grid size for ISCCP-H, the cloud amount distribution is more "U-shaped" – more near zero or near 100% cloud cover; consequently the completely clear RFO increased going from WS12 to CLR. The polar WS (PLR) is better isolated to the polar regions than the previous WS4. Extensive cirrus are better isolated in CIR. The tropical (DCN) and midlatitude (MDS) deep convection are better separated.

The loss of some interesting details in GWS-H suggests that further studies of regional cloudiness would benefit from further sub-dividing these WS (like in Tan *et al.* 2013). In particular, the two types of tropical deep convection (isolated plume and organized) represented by WS1/WS2 and WS3 in TWS are now combined in DCN (as they were in the GWS-D). Likewise, the detailed variation of the properties of subtropical low-level cloudiness with distance from the continental west coasts, represented by four WS-D (8, 9, 10, 11) in ETWS, now combine the thicker and higher-topped clouds into STC with some of the more scattered cumulus moved to FRW. On the other hand, the analysis of winds associated with the WS has been extended to include the direction of horizontal winds, showing clear separation between low and midlatitude low cloud types (Tselioudis *et al.* 2021). The midlatitude WS also clearly separate into the pre- and post-cold frontal types by wind direction. The shifting quantitative results that depend on domain and spatial scale encourages further more detailed dynamical investigations as originally envisioned.

TABLE: Average properties of corresponding GWS-D and GWS-H: relative frequency of occurrence (RFO, %), cloud fraction (CF, %), cloud top pressure (PC, hPa) and optical thickness (TAU).

| D: | WS1 | WS2 | WS3 | WS4 | WS5 | WS6 | WS7 | WS8 | WS9 | WS10 | WS11 | WS12 |
|---|---|---|---|---|---|---|---|---|---|---|---|---|
| RFO | 4.3 | 5.7 | 8.2 | 4.7 | 11.5 | 7.6 | 32.5 | 10.4 | 4.4 | 6.2 | 2.6 | 1.9 |
| CF | 98.8 | 96.8 | 93.4 | 91.6 | 83.4 | 76.4 | 29.8 | 61.8 | 81.2 | 83.1 | 93.3 | 0.0 |
| PC | 275 | 455 | 355 | 620 | 550 | 315 | 600 | 780 | 825 | 720 | 735 | --- |
| TAU | 12.4 | 11.0 | 3.4 | 11.2 | 3.2 | 1.6 | 4.0 | 3.0 | 6.6 | 5.0 | 11.4 | --- |

| H: | DCN | MDS | --- | PLR | MID | CIR | FRW | SHC | --- | STC | --- | CLR |
|---|---|---|---|---|---|---|---|---|---|---|---|---|
| RFO | 6.7 | 9.5 | --- | 3.0 | 6.1 | 15.9 | 37.5 | 7.6 | --- | 9.3 | --- | 4.2 |
| CF | 99.5 | 99.2 | --- | 84.5 | 97.2 | 79.9 | 40.0 | 79.6 | --- | 90.7 | --- | 0.0 |
| PC | 243 | 434 | --- | 396 | 607 | 316 | 645 | 840 | --- | 726 | --- | --- |

| | | | | | | | | | | | | |
|---|---|---|---|---|---|---|---|---|---|---|---|---|
| TAU | 10.5 | 10.4 | --- | 2.2 | 9.5 | 1.2 | 3.2 | 4.0 | --- | 6.3 | --- | --- |

ISCCP-D WS

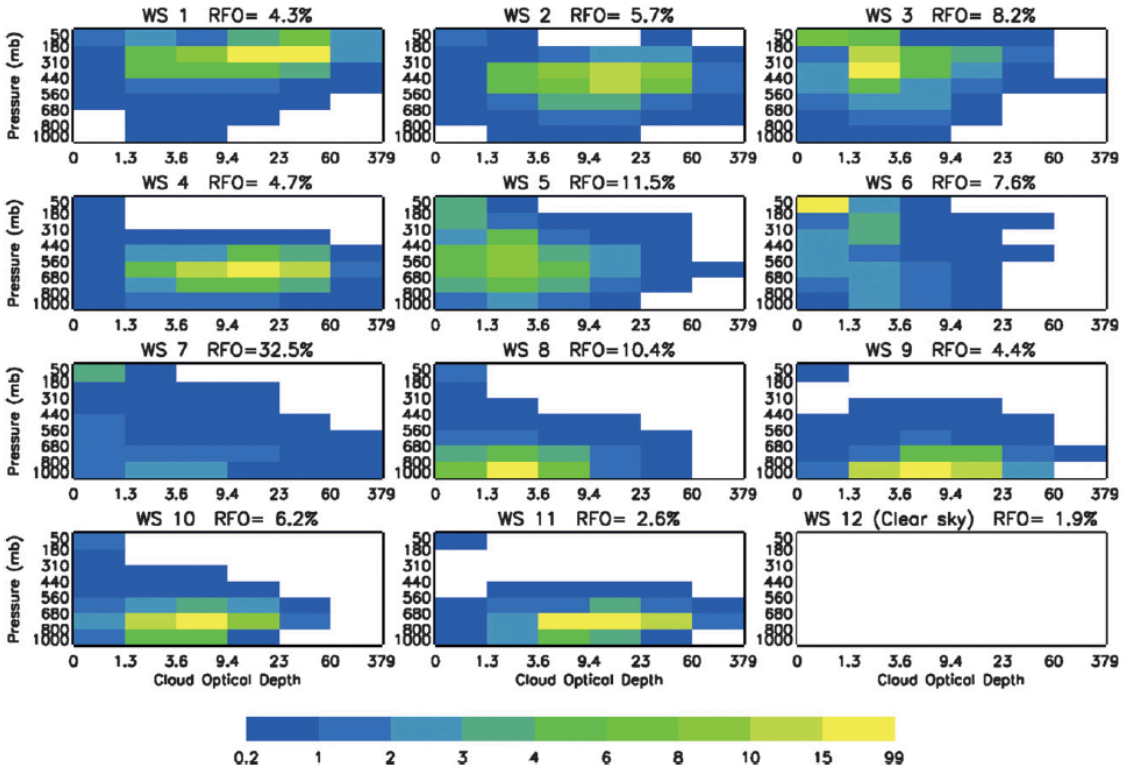
WS 1 RFO= 4.3%
WS 2 RFO= 5.7%
WS 3 RFO= 8.2%
WS 4 RFO= 4.7%
WS 5 RFO=11.5%
WS 6 RFO= 7.6%
WS 7 RFO=32.5%
WS 8 RFO=10.4%
WS 9 RFO= 4.4%
WS 10 RFO= 6.2%
WS 11 RFO= 2.6%
WS 12 (Clear sky) RFO= 1.9%
Pressure (mb)
50
180
310
440
560
680
800
1000
0 1.3 3.6 9.4 23 60 379
Cloud Optical Depth
0.2 1 2 3 4 6 8 10 15 99

ISCCP-D WS

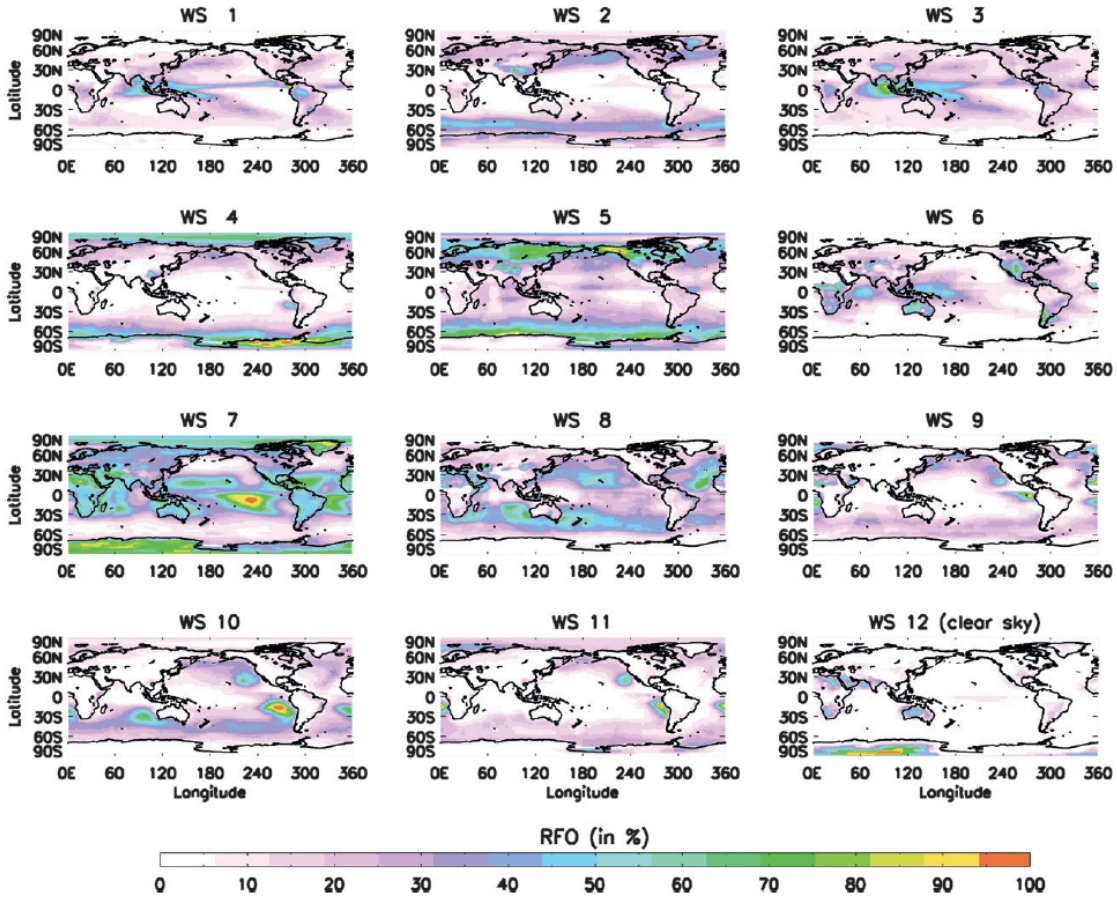
WS 1
WS 2
WS 3
WS 4
WS 5
WS 6
WS 7
WS 8
WS 9
WS 10
WS 11
WS 12 (clear sky)
Latitude
Longitude
90N
60N
30N
0
30S
60S
90S
0E
60
120
180
240
300
360
RFO (in %)
0
10
20
30
40
50
60
70
80
90
100

ISCCP-D WS

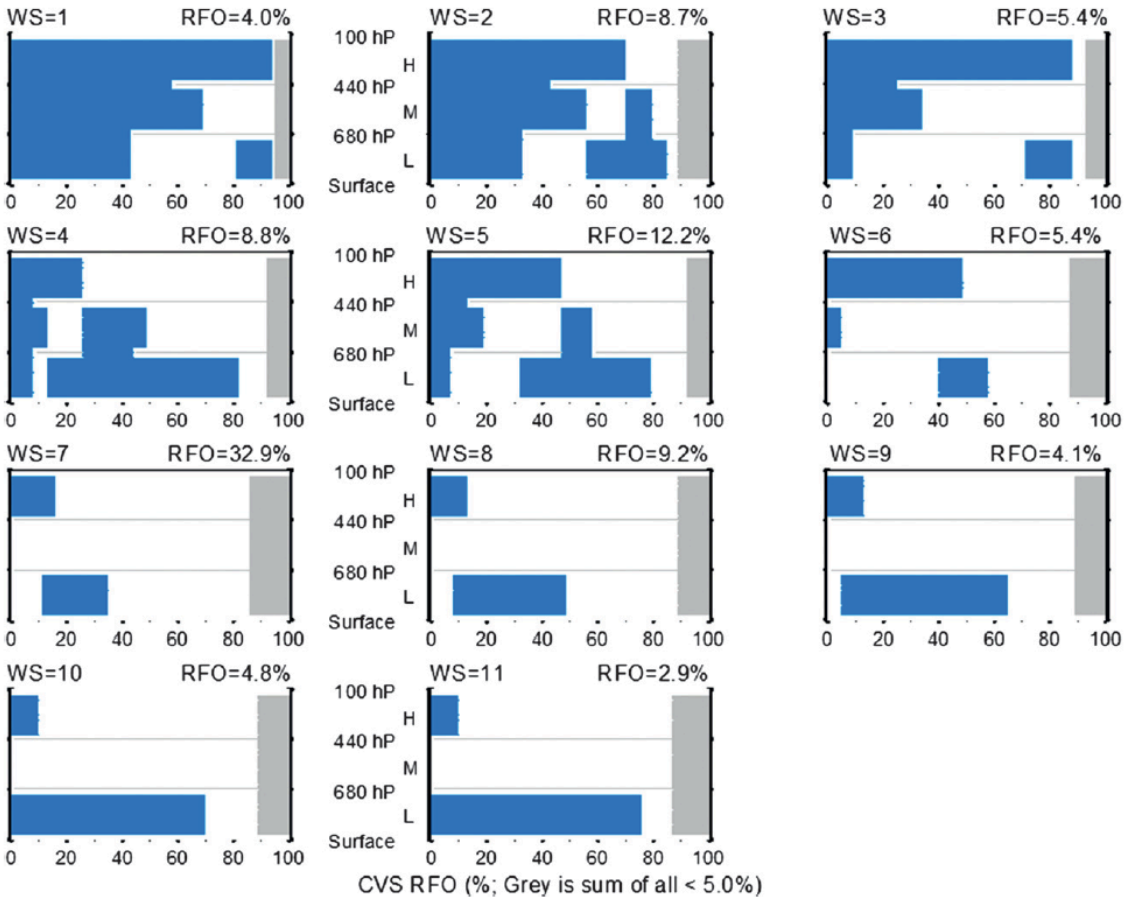
WS=1 RFO=4.0%
WS=2 RFO=8.7%
WS=3 RFO=5.4%
WS=4 RFO=8.8%
WS=5 RFO=12.2%
WS=6 RFO=5.4%
WS=7 RFO=32.9%
WS=8 RFO=9.2%
WS=9 RFO=4.1%
WS=10 RFO=4.8%
WS=11 RFO=2.9%
100 hP
440 hP
680 hP
Surface
H
M
L
0 20 40 60 80 100
CVS RFO (%; Grey is sum of all < 5.0%)

# ISCCP-H WS

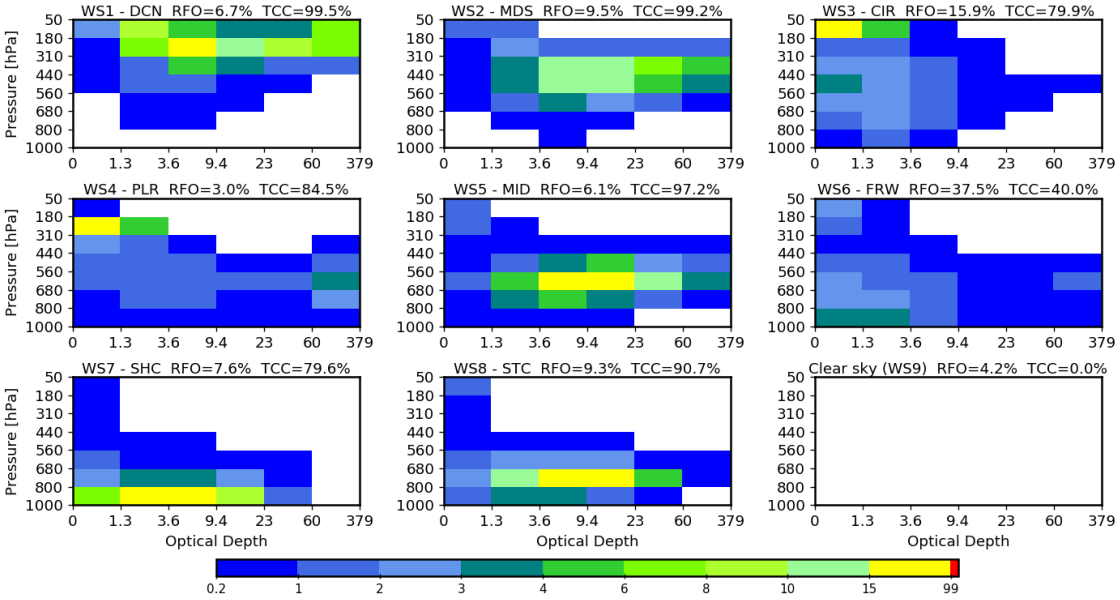
WS1 - DCN RFO=6.7% TCC=99.5%
WS2 - MDS RFO=9.5% TCC=99.2%
WS3 - CIR RFO=15.9% TCC=79.9%
WS4 - PLR RFO=3.0% TCC=84.5%
WS5 - MID RFO=6.1% TCC=97.2%
WS6 - FRW RFO=37.5% TCC=40.0%
WS7 - SHC RFO=7.6% TCC=79.6%
WS8 - STC RFO=9.3% TCC=90.7%
Clear sky (WS9) RFO=4.2% TCC=0.0%
Pressure [hPa]
50
180
310
440
560
680
800
1000
0
1.3
3.6
9.4
23
60
379
Optical Depth
0.2
1
2
3
4
6
8
10
15
99

# ISCCP-H WS

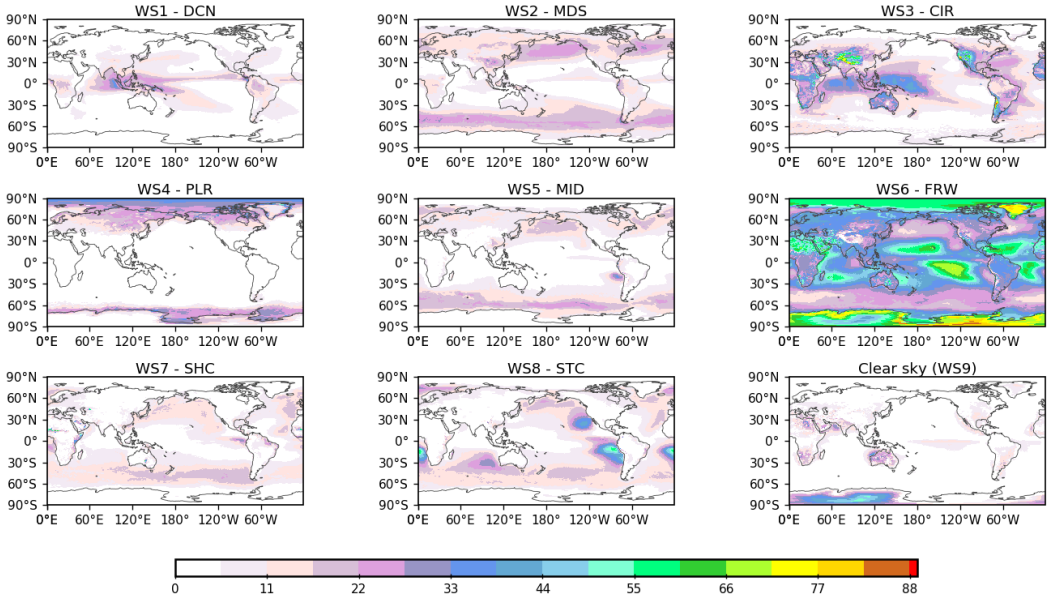
WS1 - DCN
WS2 - MDS
WS3 - CIR
WS4 - PLR
WS5 - MID
WS6 - FRW
WS7 - SHC
WS8 - STC
Clear sky (WS9)
90°N
60°N
30°N
0°
30°S
60°S
90°S
0°E 60°E 120°E 180° 120°W 60°W
0 11 22 33 44 55 66 77 88

ISCCP-H WS

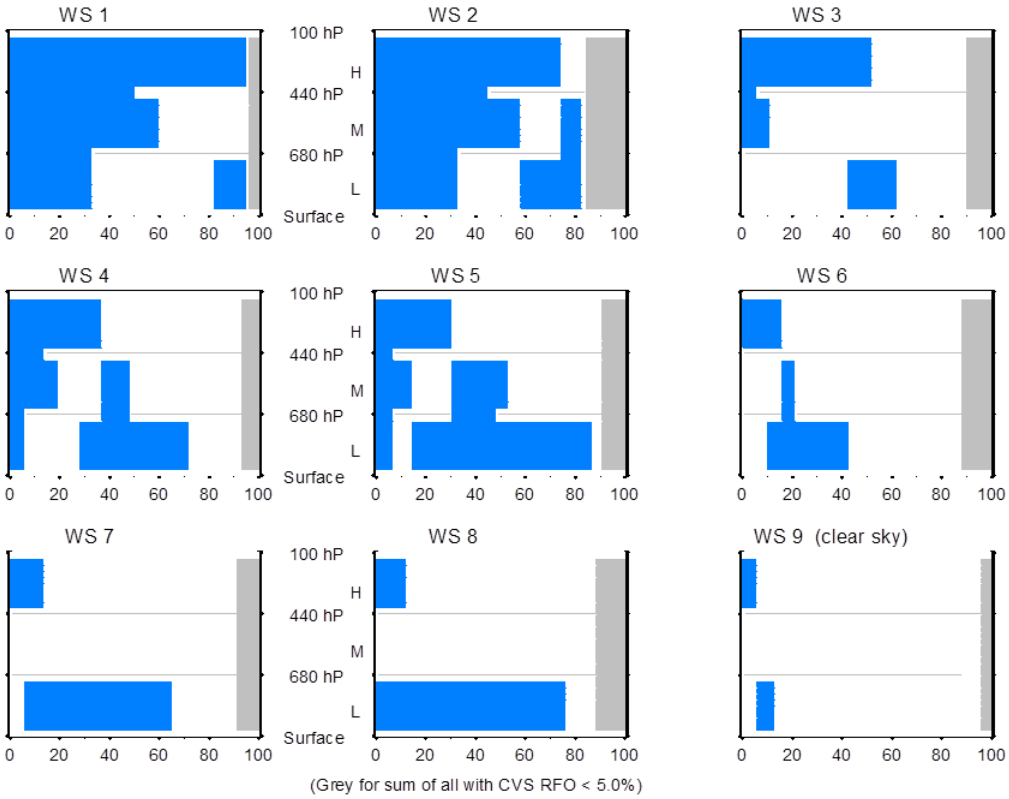


Many more analyses along these lines can be done with the datasets already available.

(1) If the histogram sample size can be increased from the ISCCP-H histograms, by constructing them on larger spatial domains (2º for instance) or over the whole daytime period, the existing WS could be sub-divided for more detailed properties (*e.g.*, Tan *et al.* 2013) or to discriminate regional differences (Leinonen *et al.* 2016). Some topics to be investigated are further elucidation of the types of deep convection (isolated plumes, mesoscale-organized, tropical and midlatitude frontal), of within-cyclone structures (tropical, extratropical), and of seasonal differences related to cloud/precipitation phase.

(2) Tracking the Lagrangian time evolution of different storms using the associated diabatic heating of the WS could characterize cloud process dynamical feedbacks.

(3) Alternate WS definitions should be investigated since the PC-TAU version mixes a physical and a radiative cloud attribute. Possibilities are PC-WP (cloud top pressure, water path) or TC-TAU (cloud top temperature, optical thickness). In addition other combinations of quantities might be informative, for example WP-Precip or WP-RH, which may diagnose precipitation onset.

(4) Composites over cloud system lifecycles of WS transitions with CloudSat-CALIPSO cloud vertical structures or TRMM precipitation profiles or microwave temperature-humidity profiles could provide more insight into cloud dynamics.

(5) Classifying the atmospheric conditions with multi-variate definitions (vertical velocity-relative humidity or freezing level) and then compositing cloud properties would complement the WS-based analyses.

(6) If sufficiently large samples can be obtained, higher dimension definitions may advance the results from the 2D WS, such as WP-RE-RH-Precip: the spatial resolution of the more advanced instruments on the AQUA satellite could provide such a combination including vertical profiles of clouds from CloudSat/CALIPSO combined with MODIS and AIRS.

REFERENCES


Anderberg, M.R., 1973: *Cluster Analysis for Applications*, 359 pp., Elsevier, New York, doi:10.1016/c2013-0-06161-0.

Arking, A., and J.D. Childs, 1985: Retrieval of cloud cover parameters from multispectral satellite measurements. *J. Climate Appl. Meteor.*, **24**, 322-333, doi:10.1175/1520-0450(1985)024<0322:roccpf>2.0.co;2.

Boccippio, D., W. Petersen and D. Cecil, 2005: The tropical convective spectrum. Part I: Archetypal vertical structures. *J. Climate*, **18**, 2744-2769, doi:10.1175/jcli3335.1.

Bodas-Salcedo, A., K. D. Williams, M. A. Ringer, I. Beau, J. N. S. Cole, J.-L. Dufrense, T. Koshiro, B. Stevens, Z. Wang, and T. Yokohata, 2014: Origins of the Solar Radiation Biases over the Southern Ocean in CFMIP2 Models. *J. Climate*, **27**, 41-56, doi:10.1175/jcli-d-13-00169.1.

Bony, S., J.L. Dufresne, H. Le Treut, J.J. Morcrette and C. Senior, 2004: On dynamic and thermodynamic components of cloud changes. *Climate Dynamics*, **22** (2-3), 71-86, doi:10.1007/s00382-003-0369-6.

Caine, S., C. Jakob, S. Siems and P. May, 2009: Objective classification of precipitating convective regimes using a weather radar in Darwin, Australia. *Mon. Wea. Rev.*, **137**, 1585-1600, doi:10.1175/2008mwr2532.1.

Chen and A.D. Del Genio, 2009: Evaluation of tropical cloud regimes in observations and a general circulation model. *Climate Dyn.*, **32**, 355-369, doi:10.1007/s00382-008-0386-6.

Desbois, M., G. Seze and G. Szejwach, 1982: Automatic classification of clouds on METEOSAT imagery: Application to high-level clouds. *J. Appl. Meteor.*, **21**, 401-412, doi:10.1175/1520-0450(1982)021<0401:acocom>2.0.co;2.

Desbois, M., and G. Seze, 1984: Use of space and time sampling to produce representative satellite cloud classifications. *Ann. Geophys.*, **2** (5), 599-606.

England, C.F., and G.E. Hunt ,1985: A bispectral method for automatic determination of parameters for use in imaging satellite cloud retrievals. *Int. J. Remote Sensing*, **6**, 1545-1553, doi:10.1080/01431168508948300.

Evans, S.M., R.T. Marchand, T.P. Ackerman and N. Beagley, 2012: Identification and analysis of atmospheric states and associated cloud properties for Darwin, Australia. *J. Geophys. Res.*, **117**, D06204, (1-12), doi:10.1029/2011jd017010.

Fereday, D.R., J.R. Knight, A.A. Scaife, C.K. Folland and A. Philipp, 2008: Cluster analysis of north Atlantic-European circulation types and links with tropical Pacific sea surface temperatures. *J. Climate*, **21**, 3687-3703, doi:10.1175/2007jcli1875.1.

Fu, R., A.D. Del Genio and W.B. Rossow, 1990: Behavior of deep convective clouds in the tropical Pacific deduced from ISCCP radiance data. *J. Climate*, **3**, 1129-1152, doi:10.1175/1520-0442(1990)003<1129:bodcci>2.0.co;2.

Gryspeerdt, E., P. Stier and D.G. Partridge, 2014: Satellite observations of cloud regime development: The role of aerosol processes. *Atmos. Chem. Phys.*, **14**(3), 1141-1158, doi:10.5194/acp-14-1141-2014.

Gordon, N.D., J.R. Norris, C.P. Weaver and S.A. Klein, 2005: Cluster analysis of cloud regimes and characteristic dynamics of midlatitude synoptic systems in

observations and a model. *J. Geophys. Res.*, **110**, D15S17, doi:10.1029/2004jd005027.
Hahn, C.J., W.B. Rossow and S.G. Warren, 2001: ISCCP cloud properties associated with standard cloud types identified in individual surface observations. *J. Climate*, **14**, 11-28, doi:10.1175/1520-0442(2001)014<0011:icpaws>2.0.co;2.
Handlos, Z.J., and L.E. Back, 2014: Estimating vertical motion profile shape within tropical weather states over the oceans. *J. Climate*, **27**, 7667-7686, doi:10.1175/jcli-d-13-00602.1.
Haynes, J.M., C. Jakob, W.B. Rossow, G. Tselioudis and J. Brown, 2011: Major characteristics of southern ocean cloud regimes and their effects on the energy budget. *J. Climate*, **24**, 5061-5080, doi:10.1175/2011jcli4052.1.
Inoue, T., 1987: A cloud type classification with NOAA-7 split-window measurements. *J. Geophys. Res.*, **92**, 3991-4000, doi:10.1029/jd092id04p03991.
Inoue, T., D. Vila, K. Rajendran, A. Hamada, X. Wu and L.A. Machado, 2009: Lifecycle of deep convective systems over the eastern tropical Pacific observed by TRMM and GOES-W. *J. Meteor. Soc. Japan*, **87**, 381-391, doi:10.2151/jmsj.87a.381.
Jakob, C., and G. Tselioudis, 2003: Objective identifications of cloud regimes in the Tropical Western Pacific. *Geophys. Res. Lett.*, **30**, 2082-2086, doi:10.1029/2003gl018367.
Jakob, C., G. Tselioudis and T. Hume, 2005: The radiative, cloud, and thermodynamic properties of the major tropical western Pacific cloud regimes. *J. Climate*, **18**, 1203-1215, doi:10.1175/jcli3326.
Jakob, C., and C. Schumacher, 2008: Precipitation and latent heating characteristics of the major tropical western Pacific cloud regimes. *J. Climate*, **21**, 4348-4364, doi:10.1175/2008jcli2122.1.
Jin, D., L. Oreopoulos and D. Lee, 2017: Regime-based evaluation of cloudiness in CMIP5 models. *Climate Dyn.*, **48**, 89-112, doi:10.1007/s00382-016-3064-0.
Jin, D., L. Oreopoulos, D. Lee, J. Tan and K. Kim, 2020: Large-scale characteristics of tropical convective systems through the prism of cloud regime. *J. Geophys. Res.*, **125**, (1-21), doi:10.1029/2019jd031157.
Kato, S., K-M. Xu, T. Wong, N.G. Loeb, F.G. Rose, K.E. Trenberth and T.J. Thorsen, 2016: Investigation of the residual in column-integrated atmospheric energy balance using cloud objects. *J. Climate*, **29**, 7435-7452, doi:10.1175/jcli-d-15-0782.1.
Lau, N-C., and M.W. Crane, 1995: A satellite view of the synoptic-scale organization of cloud properties in midlatitude and tropical circulation systems. *Mon. Wea. Rev.*, **123**, 1984-2006, doi:10.1175/1520-0493(1995)123<1984:asvots>2.0.co;2.
Lau, N-C., and M.W. Crane, 1997: Comparing satellite and surface observations of cloud patterns in synoptic-scale circulations. *Mon. Wea. Rev.*, **125**, 3172-3189, doi:10.1175/1520-0493(1997)125<3127:csasoo>2.0.co;2.
Lee, D., L. Oreopoulos, G.J. Huffman, W.B. Rossow and I-S. Kang, 2013: The precipitation characteristics of ISCCP topical weather states. *J. Climate*, **26**, 772-788, doi:10.1175/jcli-d-11-00718.1.
Leinonen, J., M.D Lebsock, L. Oreopoulos and N. Cho, 2016: Interregional differences in MODIS-derived cloud regimes. *J. Geophys. Res. Atm.*, **121**, 11648-11665, doi:10.1002/2016jd025193.

Li, W., C. Schumacher and S.A. MacFarlane, 2013: Radiative heating of the ISCCP upper level cloud regimes and its impacts on the large-scale tropical circulation. *J. Geophys. Res. Atm.*, **118**, 592-604, doi:10.1002/jgrd.50114.

Li, Y., D.W.J. Thompson, G.L. Stephens and S. Bony, 2014: A global survey of the instantaneous linkages between cloud vertical structure and large-scale climate. *J. Geophys. Res. Atmos.*, **119**, 3770-3792, doi:10.1002/2013jd020669.

Liu, G., J.A. Curry and R-S. Sheu, 1995: Classification of clouds over the western equatorial Pacific Ocean using combined infrared and microwave satellite data. *J. Geophys. Res. Atmos.*, **100**, 13811-13826, doi:10.1029/95jd00823.

Lorenz, E.N., 1984: Irregularity: A fundamental property of the atmosphere. *Tellus*, **36A**, 98-110, doi:10.1111/j.1600-0870.1984.tb00230.x.

Luo, Z.J., R.C. Anderson, W.B. Rossow and H. Takahashi, 2017: Tropical cloud and precipitation regimes as seen from near-simultaneous TRMM, CloudSat and CALIPSO observations and comparison with ISCCP. *J. Geophys. Res. Atm.*, **122**, 5988-6003, doi:10.1002/2017jd026569.

Mace, G.G., and F.J. Wrenn, 2013: Evaluation of the hydrometeor layers in the East and West Pacific within ISCCP cloud-top pressure-optical depth bins using merged CloudSat and CALIPSO data. *J. Climate*, **26**(23), 9429-9444, doi:10.1175/jcli-d-12-00207.1.

Malavelle, F.F., J.M. Haywood, A. Jones, A. Gettelman, L. Carisse, S. Boudin *et al.*, 2017: Strong constraints on aerosol-cloud interactions from volcanic eruptions. *Nature*, **546**, 485-491, doi:10.1038/nature22974.

Marchand, R., N. Beagley, S.E. Thompson, T.P. Ackerman and D.M. Schultz, 2006: A bootstrap technique for testing the relationship between local-scale radar observations of cloud occurrence and large-scale atmospheric fields. *J. Atmos. Sci.*, **63**, 2813-2830, doi:10.1175/jas3772.1.

Marchand, R., N. Beagley and T.P. Ackerman, 2009: Evaluation of hydrometeor occurrence profiles in the Multiscale Modeling Framework Climate Model using atmospheric classification. *J. Climate*, **22**, 4557-4573, doi:10.1175/2009jcli2638.1.

Mason, S., C. Jakob, A. Protat and J. Delanoe, 2014: Characterising observed mid-topped cloud regimes associated with Southern Ocean shortwave radiation biases. *J. Climate*, **27**, 6189-6203, doi:10.1175/jcli-d-14-00139.1.

McDonald, A.J., J.J. Cassano, D. Jolly, S. Parsons and A. Schuddeboom, 2016: An automated satellite cloud classification scheme using self-organizing maps: Alternative ISCCP weather states. *J. Geophys. Res. Atmos.*, **121**, 13009-13030, doi:10.1029/2016jd025199.

McDonald, A.J., and S. Parsons, 2018: A comparison of cloud classification methodologies: Differences between cloud and dynamical regimes. *J. Geophys. Res. Atmos.*, **123**, 11,173-11,193, doi:10.1029/2018jd028595.

Mekonnen, A., and W.B. Rossow, 2011: The interaction between deep convection and easterly waves tropical North Africa: A weather state perspective. *J. Climate*, **24**, 4276-4294, doi:10.1175/2011jcli3900.1.

Mekonnen, A., and W.B. Rossow, 2018: The interaction between cloud regimes and easterly wave activity over Africa: Convective transitions and mechanisms. *Mon. Wea. Rev.*, **146**. 1945-1961, doi:10.1175/mwr-d-17-0217.1.

Michelangeli, P-A., R. Vautard and B. Legras, 1995: Weather regimes: Recurrence and quasi stationarity. *J. Atmos. Sci.*, **52**, 1237-1256, doi:10.1175/1520-0469(1995)052<1237:wrraqs>2.0.co;2.

Minnis, P., and E.F. Harrison, 1984: Diurnal variability of regional cloud and clear sky radiative parameters derived from GOES data. Part I: Analysis method. *J. Climate Appl. Meteor.*, **23**, 993-1011, doi:10.1175/1520-0450(1984)023<1032:dvorca>2.0.co;2.

Oreopoulos, L., and W.B. Rossow, 2011: The cloud radiative effects of the International Satellite Cloud Climatology Project weather states. *J. Geophys. Res.*, **116**, D12202, doi:10.1029/2010jd015472.

Oreopoulos, L., N. Cho, D. Lee, S . Kato and G.J. Huffman, 2014: An examination of the nature of MODIS cloud regimes. *J. Geophys. Res. Atm.*, **119**, 8362-8383, doi:10.1002/2013jd021409.

Oreopoulos, L., N. Cho, D. Lee and S . Kato, 2016: Radiative effects of global MODIS cloud regimes. *J. Geophys. Res. Atm.*, **121**, 2299-2317, doi:10.1002/2015jd024502.

Oreopoulos, L., N. Cho and D. Lee, 2017a: Using MODIS cloud regimes to sort diagnostic signals of aerosol-cloud-precipitation interactions. *J. Geophys. Res. Atm.*, **122**, 5416-5440, doi:10.1002/2016jd026120.

Oreopoulos, L., N. Cho and D. Lee, 2017b: New insights about cloud vertical structure from CloudSat and CALIPSO observations. *J. Geophys. Res. Atm.*, **122**, 9280-9300, doi:10.1002/2017jd26629.

Oreopoulos, L., N. Cho and D. Lee, 2020: A global survey of apparent aerosol-cloud interaction signals. . *J. Geophys. Res. Atm.*, **125**, (1-21), doi:10.1002/2019jd031287.

Phulpin, T., M. Derrien and A. Brard,1983: A two-dimensional histogram procedure to analyse cloud cover from NOAA satellite high resolution imagery. *J. Climate Appl. Meteor.*, **22**, 1332-1345, doi:10.1175/1520-0450(1983)022<1332:atdhpt>2.0.co;2.

Platt, C.M.R., 1983: On the bispectral method for cloud parameter determination from VISSR satellite data: Separating broken cloud and semitransparent cloud. *J. Climate Appl. Meteor.*, **22**, 429-439, doi:10.1175/1520-0450(1983)022<0249:otbmfc>2.0.co;2.

Polly, J., and W.B. Rossow, 2016: Distribution of midlatitude cyclone attributes based on the MCMS database. *J. Climate*, 6483-6507, doi:10.1175/jcli-d-15-0857.1.

Pope, M., C. Jakob and M.J. Reeder, 2009a: Objective classification of tropical mesoscale convective systems. *J. Climate*, **22**, 5797-5808, doi:10.1175/2009jcli2777.1.

Pope, M., C. Jakob and M.J. Reeder, 2009b: Regimes of the north Australian wet season. *J. Climate*, **22**, 6699-6715, doi:10.1175/2009jcli3057.1.

Protat, A., J. Delanoe, P.T. May, J. Haynes, C. Jakob, E. O'Conner, M. Pope and M.C. Wheeler, 2011: The variability of tropical ice cloud properties as a function of the large-scale context from ground-based radar-lidar observations over Darwin, Australia. *Atmos. Chem. Phys.*, **11**, 8363-8384, doi:10.5194/acp-11-8363-2011.

Raut, B., C. Jakob and M.J. Reeder, 2014: Rainfall changes over southwestern Australia and their relationship to the Southern Annular Model and ENSO. *J. Climate*, **27**, 5801-5813, doi:10.1175/jcli-d-13-00773.1.

Remillard, J., and G. Tselioudis, 2015: Cloud regime variability over the Azores and its application to climate model evaluation. *J. Climate*, **28**, 9707-9720, doi:10.1175/jcli-d-15-0066.1.

Rossow, W.B., L.C. Garder and A.A. Lacis, 1989: Global, seasonal cloud variations from satellite radiance measurements. Part I: Sensitivity of analysis. *J. Climate*, **2**, 419-462, doi:10.1175/1520-0442(1989)002<0419:gscvfs>2.0.co;2.

Rossow, W.B., and A.A. Lacis, 1990: Global, seasonal cloud variations from satellite radiance measurements. Part II: Cloud properties and radiative effects. *J. Climate*, **3**, 1204-1253, doi:10.1175/1520-0442(1990)003<1204:gscvfs>2.0.co;2.

Rossow, W.B., and R.A. Schiffer, 1991: ISCCP cloud data products. *Bull. Amer. Meteor. Soc*., **72**, 2-20, doi:10.1175/1520-0477(1991)072<0002:icdp>2.0.co;2.

Rossow, W.B., and B. Cairns, 1995: Monitoring changes of clouds. *Climatic Change*, **31**, 305-347, doi:10.1007/978-94-011-0323-7_11.

Rossow, W.B., and R.A. Schiffer, 1999: Advances in understanding clouds from ISCCP. *Bull. Amer. Meteor. Soc*., **80**, 2261-2287, doi:10.1175/1520-0477(1999)080<2261:aiucfi>2.0.co;2.

Rossow, W.B., Y-C. Zhang and J-H. Wang, 2005a: A statistical model of cloud vertical structure based on reconciling cloud layer amounts inferred from satellites and radiosonde humidity profiles. *J. Climate*, **18**, 3587-3605, doi:10.1175/jcli3479.1.

Rossow, W.B., G. Tselioudis, A. Polak and C. Jakob, 2005b: Tropical climate described as a distribution of weather states indicated by distinct mesoscale cloud property mixtures. *Geophys. Res. Lett.*, **32**, (1-4), doi 10.1029/2005gl024584.

Rossow, W.B., A. Mekonnen, C. Pearl and W. Goncalves, 2013: Tropical precipitation extremes. *J. Climate*, **26**, 1457-1466, doi: 10.1175/jcli-d-11-00725.1.

Rossow, W.B., Y-C. Zhang and G. Tselioudis, 2016: Atmospheric diabatic heating in different weather states and the general circulation. *J. Climate*, **29**, 1059-1065, doi:10.1175/jcli-d-15-0760.1.

Rossow, W.B., K.R. Knapp and A.H. Young, 2022: International Satellite Cloud Climatology Project: Extending the record. *J Climate*, **35**. 141-158, doi:10.1175/jcli-d-21-0157.1.

Schuddeboom, A., A.J. McDonald, O. Morgenstern, M. Harvey and S. Parsons, 2018: Regional regime-based evaluation of present-day general circulation model cloud simulations using self-organizing maps. *J. Geophys. Res. Atmos.*, **123**, 4259-4272, doi:10.1002/2017jd028196.

Seze, G., and M. Desbois, 1987: Cloud cover analysis from satellite imagery using spatial and temporal characteristics of the data. *J. Climate Appl. Meteor.*, **26**, 287-303, doi:10.1175/1520-0450(1987)026<0287:ccafsi>2.0.co;2.

Shenk, W.F., and V.V. Salomonson, 1972: A multispectral technique to determine sea surface temperature using NIMBUS 2 data. *J. Phys. Oceanogr.*, **2**, 157-167, doi:10.1175/1520-0485(1972)002<0157:amttds>2.0.co;2.

Shenk, W.F., R.J. Holub and R.A. Neff, 1976: A multispectral cloud type identification method developed for tropical ocean areas with NIMBUS 3 MRIR measurements. *Mon. Wea. Rev.*, **104**, 284-291, doi:10.1175/1520-0493(1976)104<0284:amctim>2.0.co;2.

Simmer, C., E. Raschke and E. Ruprecht, 1970: A method for determination of cloud properties from two-dimensional histograms. *Ann. Meteor.*, **18,** 130-132.

Smyth, P., K. Ide and M. Ghil, 1999: Multiple regimes in northern hemisphere height fields via mixture modeling clustering. *J. Atmos. Sci.*, **56**, 3704-3723, doi:10.1175/1520-0469(1990)056<3704:mrinhh>2.0.co;2.

Stachnik, J.P., C. Schumacher and P.E. Ciesielski, 2013: Total heating characteristics of the ISCCP tropical and subtropical cloud regimes. *J. Climate*, **26**, 7097-7116, doi:10.1175/jcli-d-12-00673.1.

Stamm, A.J., and T.H. Vonder Haar, 1970: A study of cloud distributions using reflected radiance measurements from ATS satellites. *J. Appl. Meteor.*, **9**, 498-507, doi:10.1175/1520-0450(1970)009<0498:asocdu>2.0.co;2.

Su, H., J.H. Jiang, D.G. Vane and G.L. Stephens, 2008: Observed vertical structure of tropical oceanic clouds sorted in large-scale regimes. *Geophys. Res. Lett.*, **35**, 6, doi:10.029/2008gl035888.

Tan, J., and C. Jakob, 2013: A three-hourly dataset of the state of tropical convection based on cloud regimes. *Geophys. Res. Lett.*, **40**, 1415-1419, doi:10.1002/grl.50294.

Tan, J., C. Jakob and T.P. Lane, 2013: On the identification of the large-scale properties of tropical convection using cloud regimes. *J. Climate*, **26**, 6618-6632, doi:10.1175/jcli-d-12-00624.1.

Tan, J., C. Jakob, W.B. Rossow and G. Tselioudis, 2015: The role of organized deep convection in explaining observed tropical rainfall changes. *Nature*, **519**, 451-454. doi:10.1038/nature14339.

Tan, J., L. Oreopoulos, C. Jakob and D. Jin, 2018: Evaluating rainfall errors in global climate models through cloud regimes. *Climate Dyn.*, **50**, 3301-3314, doi:10.1007/s00382-017-3806-7.

Tan, J., and L. Oreopoulos, 2019: Subgrid precipitation properties of mesoscale atmospheric systems represented by MODIS cloud regimes. *J. Climate*, **32**, 1797-1812, doi:10.1175/jcli-d-18-0570.1.

Tromeur, E., and W.B. Rossow, 2010: Interaction of tropical deep convection with the large-scale circulation in the Madden-Julian oscillation. *J. Climate*, **23**, 1837-1853, doi:10.1175/202009jcli3240.1.

Tselioudis, G., Y-C. Zhang and W.B. Rossow, 2000: Cloud and radiation variations associated with northern midlatitude low and high sea level pressure regimes. *J. Climate*, **13**, 312-327, doi:10.1175/1520-0442(2000)013<0312:carvaw>2.0.co;2.

Tselioudis, G., E. Tromeur, W.B. Rossow and C.S. Zerefos, 2010: Decadal changes in tropical convection and possible effects on stratospheric water vapor. *Geophys. Res. Lett.*, **37**, L14806, (1-4), doi:10.1029/2010gl044092.

Tselioudis, G., and W.B. Rossow, 2011: Time scales of variability of the tropical atmosphere derived from cloud-defined weather states. *J. Climate*, **24**, 602-608, doi:10.1175/2010jcli3574.1.

Tselioudis, G., W.B. Rossow, Y-C. Zhang and D. Konsta, 2013: Global weather states and their properties from passive and active satellite cloud retrievals. *J. Climate*, **26**, 7734-7746, doi:10.1175/jcli-d-13-00024.1.

Tselioudis, G., W.B. Rossow, C. Jakob, J. Remillard, D. Tropf and Y-C. Zhang, 2021: Evaluation of clouds, radiation, and precipitation in CMIP6 models using global weather states derived from ISCCP-H cloud property data, *J. Climate,* **34**, 7311-7324, doi:10.1175/jcli-d-21-0076.1.

Tsushima, Y., M.A. Ringer, M.J. Webb and K.D. Williams, 2013: Quantitative evaluation of the seasonal variations of climate model cloud regimes. *Climate Dyn.*, doi:10.1007/s00382-012-1609-4.

Unglaub, C., K. Block, J. Mulmenstadt, O. Sourdeval and J. Quaas, 2020: A new classification of satellite-derived liquid water cloud regimes at cloud scale. *Atmos. Chem. Phys.*, **20**, 2407-2418, doi:10.5194/acp-20-2407-2020.

Vonder Haar, T.H., 1970: Application of simultaneous infrared radiance measurements and cloud photographs from satellites. *J. Appl. Meteor.*, **9**, 955-958, doi:10.1175/1520-0450(1970)009<0955:aosirm>2.0.co;2.

Williams, K.D., and G. Tselioudis, 2007: GCM intercomparison of global cloud regimes: Present-day evaluation and climate change response. *Climate Dyn.*, **29** (2-3), 231-250, doi:10.1007/s00382-007-0232-2.

Williams, K.D., and M.E. Brooks, 2008: Initial tendencies of cloud regimes in the Met Offie Unified Model. *J. Climate*, **21**, 833-840, doi:10.1175/2007jcli1900.1.

Williams, K.D., and M.J. Webb, 2009: A quantitative performance assessment of cloud regimes in climate models. *Climate Dyn.*, **33** (1), 141-157, doi:10.1007/s00382-008-0443-1.

Williams, K.D., and A. Bodas-Salcedo, 2017: A multi-diagnostic approach to cloud evaluation. *Geosci. Model Devel. Disc.*, **2017**, 1-44, 10.5194/gmd-2016-295.

Worku, L.Y., A. Mekonnen and C.J. Schreck, 2019: Diurnal cycle of rainfall and convection over Maritime Continent using TRMM and ISCCP. *Int. J. Climatol.*, 1-10, doi:10.1002/joc6121.

Worku, L.Y., A. Mekonnen and C.J. Schreck, 2020: The impact of MJO, Kelvin, Equatorial Rossby waves on the diurnal cycle over the Maritime Continent. *Atmosphere*, **2020**, 11, 711, doi:10.3390/atmos11070711.

Young, A.H., K.R. Knapp, A. Inamdar, W. Hankins and W.B. Rossow, 2018: The International Satellite Cloud Climatology Project H-Series Climate Data Record Product. *Earth System Science Data*, **10**, 583-593, doi:10.5194/essd-10-583-2018.

Yuter, S.E., and R.A. Houze, 1995: Three-dimensional kinematic and microphysical evolution of Florida cumulonimbus, part II: Frequency distributions of vertical velocity, reflectivity and differential reflectivity. *Mon. Wea. Rev.*, **123**, 1941-1963, doi:10.1175/1520-0493(1995)123<1941:tdkame>2.0.co;2.

Zhang, Y., S. Klein, G.G. Mace and J. Boyle, 2007: Cluster analysis of tropical clouds using CloudSat data. *Geophys. Res. Lett.*, **34**, L12813, (1-4), doi:10.1029/2007gl029336.